

# Application of the physics of plasma sheaths to the modeling of rf plasma reactors

A. Metze,<sup>a)</sup> D. W. Ernie, and H. J. Oskam

Department of Electrical Engineering, University of Minnesota, Minneapolis, Minnesota 55455

(Received 16 June 1986; accepted for publication 22 July 1986)

An equivalent circuit model is presented for a planar rf plasma reactor. The physical properties of the plasma sheath adjacent to the electrodes are incorporated in the model. The sheath capacitances and the conduction currents through the sheaths are time varying and have a highly nonlinear dependence on the potentials across the plasma sheaths. The model shows that the waveforms of the voltage differences across the sheaths are highly nonsinusoidal and agree with reported measurements.

## I. INTRODUCTION

The application of rf-excited gaseous discharges in thin-film fabrication technology has become standard during the past decade. The simplest geometry most commonly used is that of two planar electrodes between which the rf voltage is applied.<sup>1</sup> A schematic representation of such a planar rf plasma reactor is shown in Fig. 1. The plasma is separated from each electrode by a plasma sheath. The origin of these plasma sheaths has been discussed by several authors.<sup>2,3</sup>

Positive ions produced in the plasma volume are accelerated across the plasma sheaths and arrive at the electrodes with an energy distribution which is determined by the magnitude and the waveform of the time-dependent potential difference across the sheaths, the gas pressure, etc. This ion bombardment energy distribution determines the degree of anisotropy in thin-film etching, amount of ion impact induced damage to surfaces, etc. Therefore, it is important to obtain a better understanding of the dependence of the ion bombardment energy distribution on parameters such as reactor geometry, frequency of the applied voltage, gas pressure, etc. Suzuki *et al.*<sup>4</sup> and Tsui<sup>5</sup> have reported models relating to the energy distribution of positive ions arriving at the electrodes of a rf plasma reactor. These authors assumed that the electric potential difference across the plasma sheath is simply the superposition of a dc bias and a sinusoidal voltage.

In order to obtain a more accurate model for the ion bombardment energy distribution, it is necessary to develop a model which predicts the waveforms of the voltages across the plasma sheaths in a planar rf plasma reactor. In an effort to determine these waveforms, several authors have used a combination of circuit elements for the representation of the plasma sheaths in equivalent circuit models of a planar plasma reactor. Koenig and Maissel<sup>6</sup> used a static capacitor in parallel with a diode. The capacitor represented the sheath capacitance, while the diode approximated the effect of electrons reaching the electrodes. Horwitz<sup>7</sup> added a parallel resistor to the previous model, while other authors have used a simple parallel combination consisting of a resistor and capacitor of fixed values.<sup>8,9</sup> The latter model is sometimes further simplified by a purely linear resistive network for

excitation frequencies below a few megahertz and by a purely linear capacitive network for higher frequencies.<sup>9,10</sup>

The purpose of the present paper is to demonstrate that an equivalent circuit model of a plasma reactor can be developed using known physical properties of plasma sheaths. The main feature of the proposed model is the inclusion of the nonlinear dependence of the sheath properties on the voltage across the sheath. The purpose of the model is to evaluate the effects of the nonlinear sheath properties on the resulting voltage waveforms and the dc voltage biases across the plasma sheaths. The resulting sheath voltage waveforms can then be used to more accurately predict the ion bombardment energy distribution at the surface of the electrodes in a planar rf plasma reactor.

## II. MODEL OF THE PLASMA SHEATH IN A PLANAR rf GASEOUS DISCHARGE

The schematic representation of a planar plasma sheath used in the following discussion is shown in Fig. 2. During the discussion of the sheath properties the Bohm<sup>11</sup> criterium will be used. This criterion implies that, for a surface biased strongly negative with respect to a plasma, the ions are accelerated across a pre-sheath by the applied electric field such that they enter the plasma sheath with a velocity perpendicular to the sheath boundary and with a magnitude equal to or greater than  $(kT_e/M)^{1/2}$ . Here,  $k$  is Boltzmann's constant,  $M$  is the ion mass, and  $T_e$  is the electron temperature.

Several assumptions will be made in order to simplify the present discussion. Refinements of the model can be in-

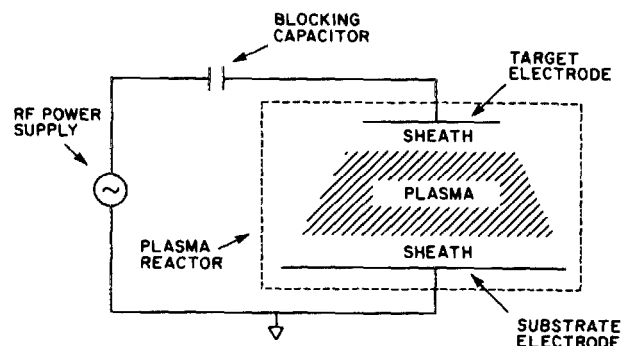


FIG. 1. Schematic representation of a planar rf reactor.

<sup>a)</sup> Present address: Honeywell Systems and Research Center, 3660 Technology Drive, Minneapolis, MN 55418.

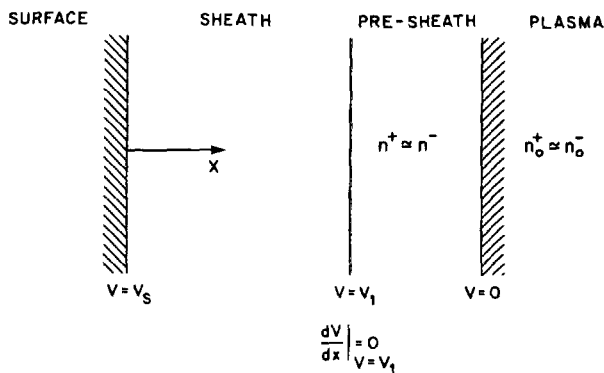


FIG. 2. Schematic representation of a planar plasma sheath.

cluded in future discussions. The assumptions used for the present model are the following:

(1) The charged particles are electrons and one type of positive ions. The presence of more than one type of positive ion will only slightly modify the model presented. In many applications of plasma processing of materials electronegative gases are used. Plasmas produced in these gases will contain negative ions. The presence of negative ions is excluded in the present model since an accurate incorporation of these ions complicates the model of the plasma sheath. However, as long as the negative ion density inside the plasma sheath is small compared to that of the positive ion density, the present model is a good approximation.

(2) The electrons and ions have Maxwellian velocity distributions inside the plasma with temperatures of  $T_e$  and  $T_i$ , respectively.

(3) The electron temperature  $T_e$  is constant in time, while the ion temperature  $T_i$  is equal to the constant neutral gas temperature  $T_g$ . The assumption of constant  $T_e$  limits the model to a minimum frequency of the applied power source. The numerical calculations presented in this paper for a planar plasma reactor are for a plasma produced in argon. For these conditions, the energy modulation of the majority of the electrons is small for frequencies larger than approximately 50 kHz and gas pressures smaller than approximately 1 Torr.<sup>12</sup>

(4) The electron and ion densities inside the plasma volume are constant in time. The validity of this assumption depends on the rate of loss of the charged particles from the plasma volume as well as on the mechanism by which the plasma is maintained. The charged particle density modulation due to loss by ambipolar diffusion in a plasma reactor is small for frequencies larger than approximately 50 kHz and pressures larger than approximately 0.1 Torr.<sup>13</sup> The periodic charged particle current across the plasma sheaths towards the electrodes is governed by the properties of the plasma sheath. The model shows that this number loss of charged particles is small compared to the charge particle density inside the plasma, since only a relatively small fraction of the plasma electrons and ions is able to reach the electrodes.

The modulation in the rate of production of charged particles depends on the maintenance mechanism of the discharge plasma. For instance, if the plasma electrons (ions) are mainly produced by secondary electrons emitted due to ion bombardment of the electrodes, the rate of charged parti-

cle production inside the plasma can be considerably modulated. This is caused by the energy and flux modulation of these electrons due to the time-dependence voltage difference across the plasma sheath. The possible effect of this phenomenon is not included in the present model.

(5) The influence of collisions between charged particles and neutral particles inside the plasma sheath on the charged particle motion can be neglected (collisionless sheath). For instance, this is a good assumption for the charged particle densities (sheath dimensions) and gas pressures (charged particle mean free paths) used for anisotropic etching of films in a planar rf plasma reactor.

(6) The transit time  $\tau_i$  of ions through the plasma sheath is not larger than  $1/f$ , where  $f$  is the frequency of the applied voltage. If this condition is satisfied, then the thickness of the plasma sheath will, at each time, correspond to the steady-state thickness related to the instantaneous voltage  $V_s(t)$  across the sheath. Calculations for argon ions and plasma densities of  $10^{10} \text{ cm}^{-3}$  show that  $\tau_i$  is smaller than  $0.5 \times 10^{-6} \text{ s}$ . Therefore, this assumption appears to be valid for frequencies up to approximately 1 MHz.

(7) The flux of electrons collected by the electrodes depends only on the instantaneous voltage across the plasma sheath and not on the frequency of the voltage waveform. Numerical calculations by the authors indicate that this assumption is valid for frequencies up to a few megahertz.<sup>14</sup>

(8) The Bohm sheath criterium can be used in the form that the speed with which the ions enter the plasma sheath is equal to  $(kT_e/M)^{1/2}$  and is valid for the range of voltages across the plasma sheaths of interest.<sup>15</sup>

(9) The electric field is zero at the boundary between the pre-sheath and the plasma sheath.<sup>16</sup>

(10) The electrons have a Boltzmann density distribution in the pre-sheath and the plasma sheath.<sup>17</sup>

The two quantities related to the plasma sheath which have to be included in the equivalent circuit model of a planar rf plasma reactor presented in the next section are the capacitance  $C_s$  of the plasma sheath and the conduction current  $I$  through the sheath. An expression for  $C_s$  as a function of sheath potential ( $V_s - V_1$ ) can be derived by noting that the displacement current  $I_d$  for the sheath capacitance is given by<sup>18</sup>

$$I_d = \frac{dQ}{dt} = \frac{dQ}{dV_s} \frac{dV_s}{dt} \equiv C_s \frac{dV_s}{dt}, \quad (1)$$

where  $Q$  is the surface charge on the electrode. For a planar electrode, the sheath capacitance  $C_s$  is thus given by

$$C_s \equiv \frac{dQ}{dV_s} = -\epsilon_0 \int \frac{\partial E_A}{\partial V_s} \cdot dA = -\epsilon_0 A \frac{\partial E_A}{\partial V_s}, \quad (2)$$

where  $\epsilon_0$  is the permittivity of free space and it is assumed that the electric field at the electrode surface  $E_A$  is normal to and uniform over the electrode surface with area  $A$ .

Using the mentioned assumptions, it can be shown that

$$E_A = -\left(\frac{2kT_e n_1}{\epsilon_0}\right)^{1/2} \times \left[ \exp\left(\frac{e(V_s - V_1)}{kT_e}\right) + \left(\frac{V_s}{V_1}\right)^{1/2} - 2 \right]^{1/2}$$

$$\text{for } -\infty < V_s(t) < V_1 \quad (3a)$$

$$E_A = 0 \quad \text{for } V_1 \leq V_s(t) \leq 0. \quad (3b)$$

Here,

$$V_1 = -(kT_e/2e) \quad (4)$$

and

$$n_1 = n_0 \exp(eV_1/kT_e), \quad (5)$$

where  $n_0$  is the density of electrons and ions inside the plasma. Equations (2) and (3) show that  $C_s(V_s)$  is time varying and has a strong nonlinear dependence on  $V_s(t)$ .

The assumptions made imply that the conduction current  $I(V_s)$  through the plasma sheath is given by the static plasma probe current-voltage characteristic (Langmuir probe curve) derived by including the Bohm criterium, i.e.,

$$I(V_s) = AJ_e \exp(eV_s/kT_e) + AJ_i \quad \text{for } V_s(t) \leq 0. \quad (6)$$

Here,  $A$  is the area of the electrode and the saturated charged particle current densities are

$$J_e = -en_0\bar{v}_e/4 = -en_0(kT_e/2\pi m)^{1/2} \quad (7)$$

and

$$J_i = 0.605n_0e(kT_e/M)^{1/2}, \quad (8)$$

where  $m$  and  $M$  are the electron and ion mass, respectively, and  $\bar{v}_e$  is the average electron speed inside the plasma.

The expressions given in this section for the capacitance  $C_s(V_s)$  of the plasma sheath and the conduction current  $I(V_s)$  through the plasma sheath will be used in the equivalent circuit model for a planar rf discharge presented in the following section.

### III. EQUIVALENT CIRCUIT MODEL FOR A PLANAR rf PLASMA REACTOR

A schematic of the equivalent electric circuit model used in the present discussion is shown in Fig. 3. Here,  $V_{rf}$  is the voltage of the applied rf signal from a matched rf power supply;  $V_T$  and  $V_p$  are the potentials of the target electrode and the plasma, respectively, and  $V_{ss} = V_p$  and  $V_{ST} = V_T - V_p$  are the voltages across the substrate-plasma sheath and the target-plasma sheath, respectively. The blocking capacitor is represented by  $C_B$ ;  $C_{ST}$  and  $I_T$  represent the capacitance of and conduction current through the

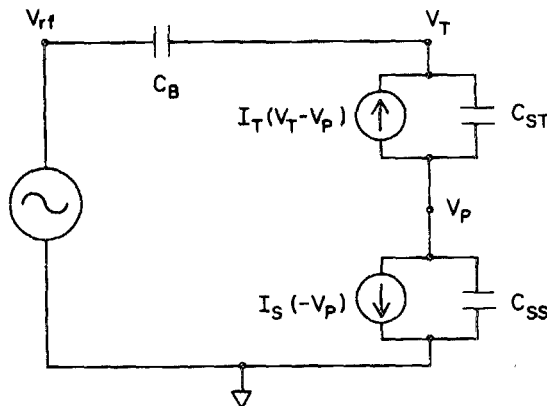


FIG. 3. Equivalent electric circuit model of a plasma reactor.

sheath adjacent to the target electrode, respectively, while  $C_{ss}$  and  $I_S$  represent the corresponding values for the sheath adjacent to the substrate electrode. The expressions for  $C_{ST}$  and  $C_{ss}$  are given by Eqs. (2) and (3), while the expressions for  $I_T$  and  $I_S$  are given by Eqs. (6), (7), and (8).

The electrical resistance of the plasma has been neglected in this circuit model. This resistance is small with respect to the sheath resistance for the plasma electron densities and voltage frequency range considered in the present discussion. However, inclusion of the plasma resistance does not introduce any complications for the circuit model.

The purpose of the model is to derive the time dependence of  $V_p$ ,  $V_T$ , the total current at the node denoted by  $V_T$ , and the conduction currents through the plasma sheaths in this circuit. From these results, quantities such as the sheath potentials as a function of time and the resulting dc self biases can also be calculated.

From this equivalent circuit model and from conservation of current at the nodes denoted by  $V_T$  and  $V_p$ , it follows that

$$C_{ST} \frac{d}{dt}(V_p - V_T) + C_B \frac{d}{dt}(V_T - V_{rf}) + I_T = 0, \quad (9a)$$

$$C_{ss} \frac{d}{dt}V_p + C_{ST} \frac{d}{dt}(V_p - V_T) + I_T + I_S = 0. \quad (9b)$$

If Eqs. (2) and (3) for  $C_s(V_s)$  and Eq. (6) for  $I(V_s)$  are used in the current continuity Eqs. (9), the set of continuity equations can be solved numerically for  $V_p(t)$  and  $V_T(t)$ . In addition, by then using these results, the current in the circuit at the node denoted by  $V_T$  and the conduction currents  $I_S$  and  $I_T$  in the plasma sheaths can be calculated.

### IV. NUMERICAL RESULTS AND DISCUSSION

Numerical simulations were performed based on the equivalent circuit model for the following assumed conditions:

- $M = 40$  amu (argon discharge),
- $n_0 = 10^{10}$  particles/cm<sup>3</sup> (charged particle density in plasma),
- $T_i = 500$  K (ion temperature),
- $T_e = 23\,200$  K (electron temperature),
- $A_T = 100\pi$  cm<sup>2</sup> (area of target electrode),
- $V_{rf} = 1000 \sin \omega t$  (applied rf voltage).

These conditions imply that

- $J_i = 214 \mu\text{A/cm}^2$  (saturated ion current),
- $J_e = -38 \text{ mA/cm}^2$  (saturated electron current),
- $V_F = -10.35$  V (floating potential).

The floating potential is the voltage difference across the plasma sheath and pre-sheath for which the total conduction current through the sheath is zero. Its value is given by

$$V_F = -(kT_e/e) \ln(-J_e/J_i), \quad (10)$$

which follows directly from Eq. (6).

Figure 4 shows the calculated waveforms for the voltage  $V_T$  across the plasma reactor and the plasma potential  $V_p$ . The calculations relate to a frequency  $f = 100$  kHz, a blocking capacitance  $C_B = 150$  pF, and an electrode area ratio  $A_T/A_s = 1.0$ , where  $A_T$  is the area of the target electrode

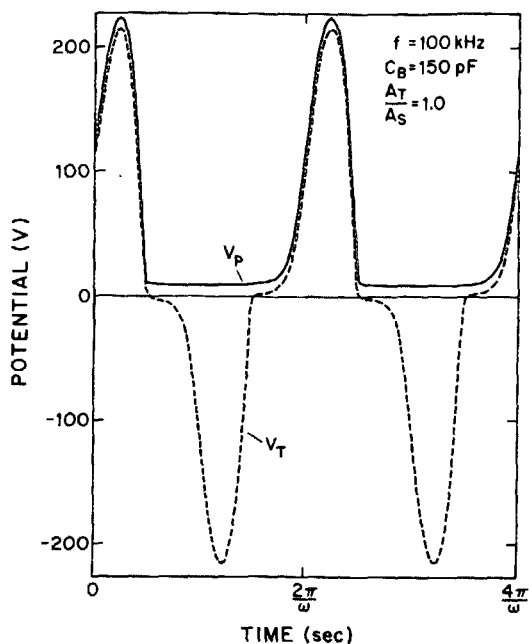


FIG. 4. Calculated waveforms of the voltage  $V_T$  across the plasma reactor and the plasma potential  $V_p$  for equal areas of the target and substrate electrodes.

and  $A_s$  is the area of the substrate electrode. The sheath voltage waveforms  $V_{ss} = -V_p$  and  $V_{st} = V_T - V_p$  are shown in Fig. 5. These calculated waveforms show that both electrodes always have a negative potential with respect to the plasma. These results are in very good agreement with measurements by Bruce.<sup>19</sup> Figure 6 shows an expanded view of the waveforms of the sheath voltages close to the floating

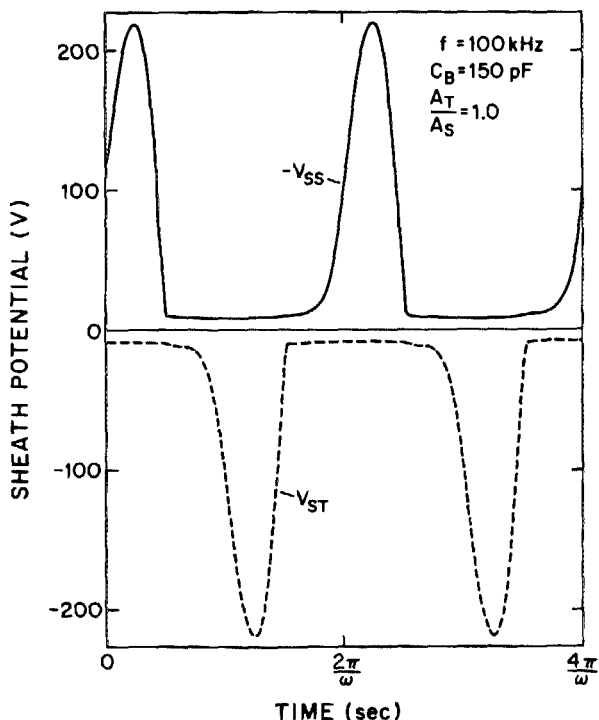


FIG. 5. Calculated waveform of the potential  $V_{ST}$  across the plasma sheath adjacent to the target electrode and that of the potential  $V_{SS}$  across the substrate electrode sheath for  $A_T/A_S = 1$ .

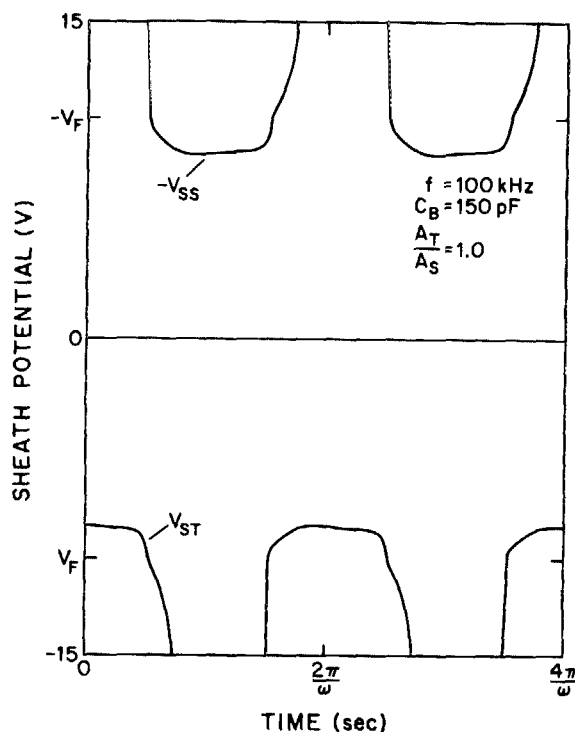


FIG. 6. Calculated sheath voltage waveforms  $V_{ST}$  and  $V_{SS}$  close to the floating potential  $V_F$  for  $A_T/A_S = 1$ .

potential  $V_F$  where it is seen that the smallest magnitude of the time dependent sheath potential is only slightly smaller than  $|V_F|$ . The nonsinusoidal nature of the sheath voltage waveforms  $V_{ss}$  and  $V_{st}$  (and, hence, of  $V_p$  and  $V_T$ ) is due to the highly nonlinear properties of the sheath capacitances  $C_{ss}$  and  $C_{st}$  and the conduction currents  $I_s$  and  $I_T$  through the plasma sheaths. At this frequency, these waveform shapes are predominantly determined by the large difference in magnitude between the saturated ion current and the larger saturated electron current and by the exponential increase of the electron current through the plasma sheath with decreasing values of  $|V_s|$ . Since no net dc current component can flow in the circuit, the magnitude of the sheath potentials need only be slightly smaller than  $|V_F|$  for part of the rf cycle, during which time sufficient net electron current flows in order to balance the net ion current which flows during the remainder of the rf cycle.

The waveform of the conduction current  $I_T$  through the sheath adjacent to the target electrode is shown in Fig. 7. This current becomes independent of the sheath voltage  $V_{ST}$  (and thus time) for large negative sheath voltages (saturated ion current only), while the contribution of the electron current only becomes important for values of  $V_{ST}$  close to the floating potential  $V_F$  (compare with Figs. 5 and 6). For this symmetrical condition ( $A_T = A_S$ ) the waveform of  $I_s$  is identical with that of  $I_T$ , but is shifted by  $\pi/\omega$  s, as can be expected. The waveform of the total current,  $I_{total}$ , through the discharge is shown in Fig. 8. This waveform is again nonsinusoidal as can be expected from the nonlinear properties of the plasma sheaths. It should also be noted that the time averages of the currents  $I_T$ ,  $I_s$ , and  $I_{total}$  are equal to zero, as is required, since no net dc current component can flow in the circuit.

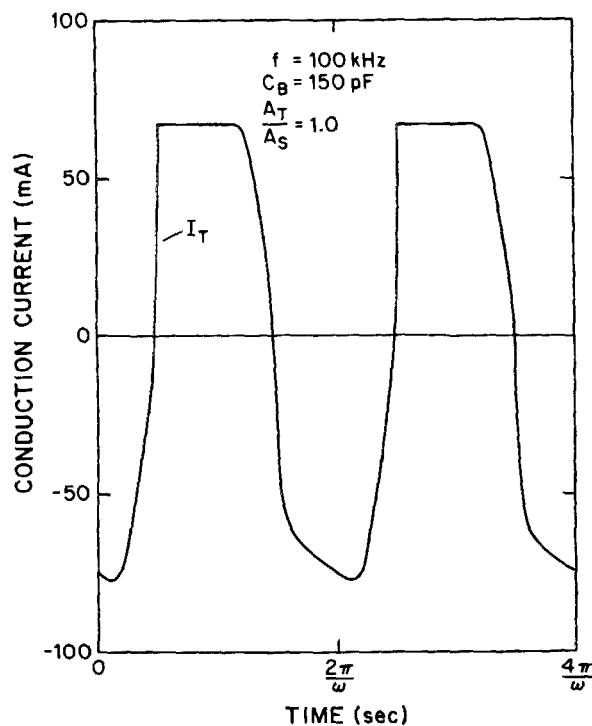


FIG. 7. Calculated waveform of the conduction current  $I_T$  through the plasma sheath adjacent to the target electrode for  $A_T/A_S = 1$ .

The next sequence of figures gives the various waveforms for an experimental condition in which the area of the substate electrode is five times the area of the target electrode ( $A_T = 100\pi \text{ cm}^2$  and  $A_S = 500\pi \text{ cm}^2$ ). The value of the blocking capacitor was slightly changed in these calculations in order to keep the voltage amplitude across the reactor,  $V_T$ , approximately the same as in the previous calculations for the symmetrical condition ( $A_T/A_S = 1$ ). Figure 9 shows

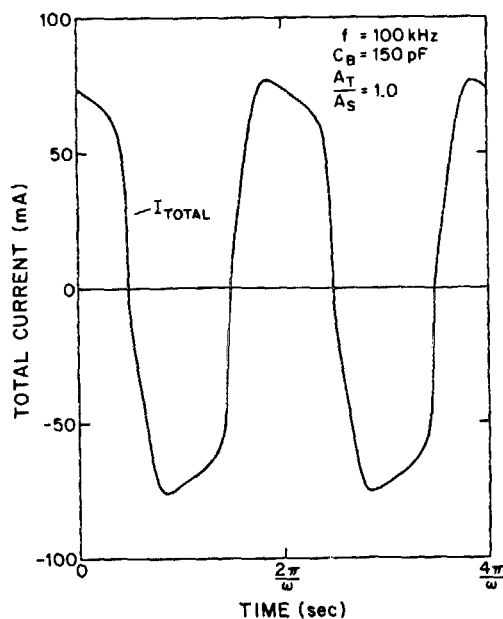


FIG. 8. Calculated waveform of the total current  $I_{\text{total}}$  through the plasma reactor for  $A_T/A_S = 1$ .

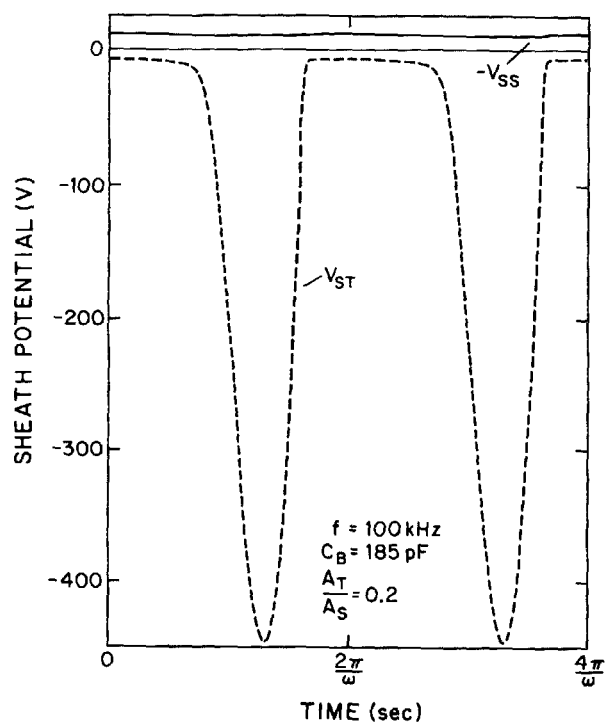


FIG. 9. Calculated waveform of the potential  $V_{ST}$  across the plasma sheath adjacent to the target electrode and that of the potential  $V_{SS}$  across the substrate electrode sheath for  $A_T/A_S = 0.2$ .

the waveforms of the sheath potentials  $V_{ST}$  and  $V_{SS}$ , while Fig. 10 shows an expanded view of these waveforms close to the floating potential  $V_F$ . The maximum value of  $|V_{ST}|$  is about twice the amplitude of the voltage,  $V_T$ , across the plasma reactor, while the value of  $V_{SS}$  remains close to the value of  $V_F$ . The latter effect is shown in more detail in Fig. 11.

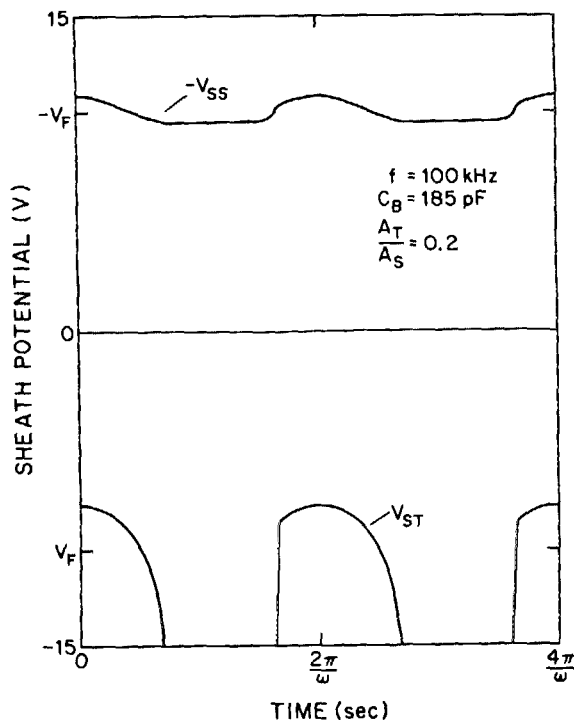


FIG. 10. Calculated sheath voltage waveforms  $V_{ST}$  and  $V_{SS}$  close to the floating potential  $V_F$  for  $A_T/A_S = 0.2$ .

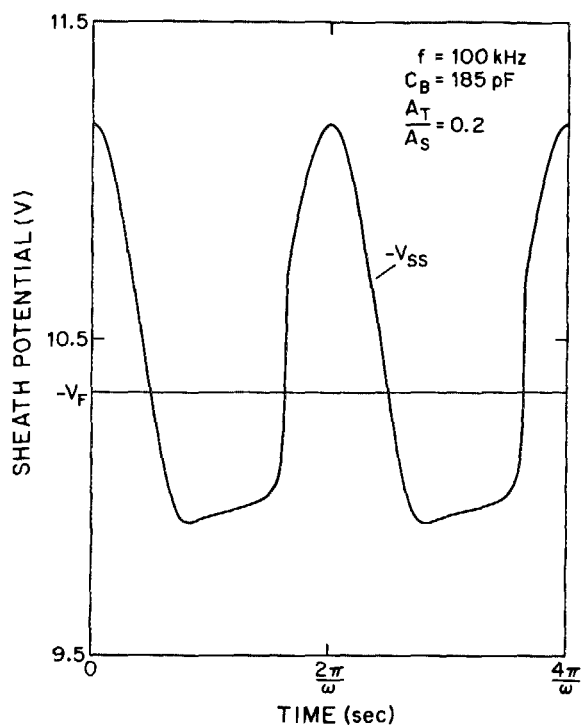


FIG. 11. Calculated sheath voltage waveform  $V_{ss}$  very close to the floating potential  $V_F$  for  $A_T/A_S = 0.2$ .

The waveforms of the conduction currents,  $I_T$  and  $I_S$ , through the two plasma sheaths are shown in Figs. 12 and 13, respectively. The waveform of  $I_T$  is analogous to that for the symmetrical configuration. However, the electron current contributes significantly to  $I_S$  during all times, since the saturated ion current at the substrate electrode is 336 mA, while at the target electrode this current is only 67 mA. The

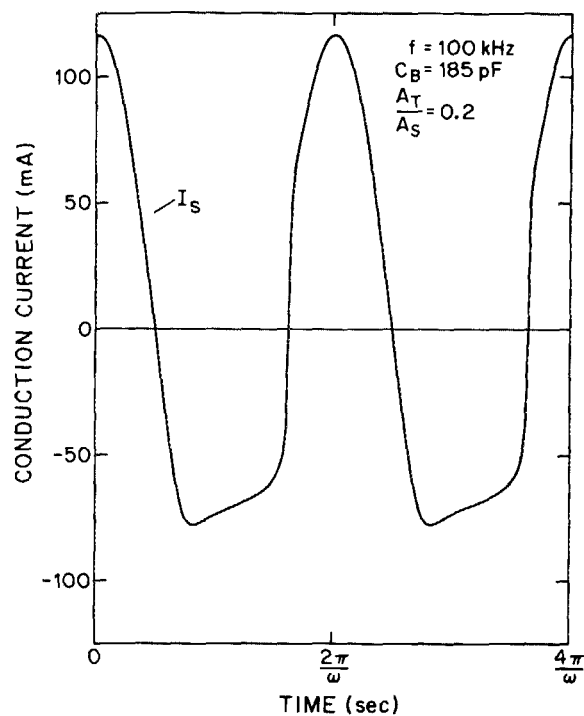


FIG. 13. Calculated waveform of the conduction current  $I_S$  through the plasma sheath adjacent to the substrate electrode for  $A_T/A_S = 0.2$ .

reason that the amplitude of  $V_{ST}$  is much larger than that of  $V_{SS}$  is the difference in electron and saturated ion currents at the two electrodes due to the difference in  $A_T$  and  $A_S$ . The variation in  $V_{ss}$  required in order to adjust  $I_S$  for the variation in  $I_T$  becomes smaller than the variation in  $V_{ST}$  as the ratio  $A_T/A_S$  becomes smaller. The waveform of the total current through the plasma reactor is shown in Fig. 14.

## V. CONCLUSIONS

The model presented is based on the inclusion of the physical properties of plasma sheaths in an equivalent circuit representation of a planar rf-excited gaseous discharge. The

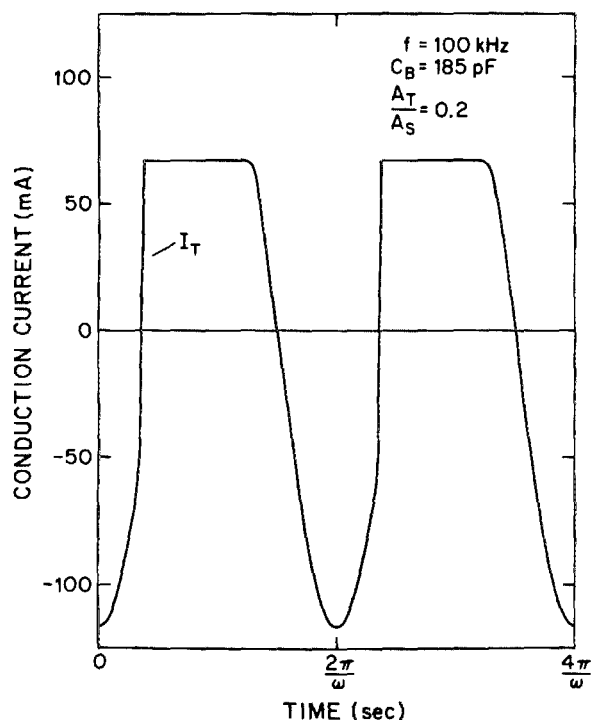


FIG. 12. Calculated waveform of the conduction current  $I_T$  through the plasma sheath adjacent to the target electrode for  $A_T/A_S = 0.2$ .

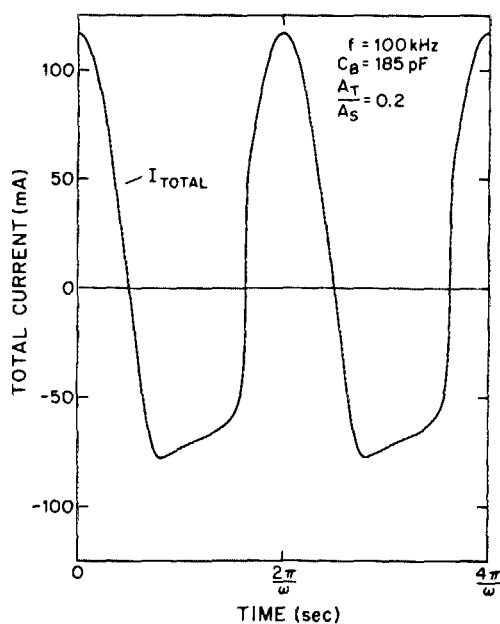


FIG. 14. Calculated waveform of the total current  $I_{total}$  through the plasma reactor for  $A_T/A_S = 0.2$ .

proposed model is valid under the assumptions made in Sec. II. The model shows that the waveforms of the voltage differences across the plasma sheaths are highly nonsinusoidal. These waveforms are in agreement with studies reported by Bruce.<sup>19</sup> The resulting current waveforms in the circuit are also highly nonsinusoidal. The waveforms of the voltage,  $V_T$ , across the reactor and of the total current,  $I_{\text{total}}$ , through the reactor have important implications when determining the power applied to the reactor. This model also shows that the relative amplitudes of the voltage waveforms across the target and substrate plasma sheaths depend on the area ratio of the electrodes, with the largest amplitude waveform across the sheath adjacent to the smallest area electrode.

The effect of the calculated nonsinusoidal waveform of the plasma sheath voltage on the energy distribution of the positive ions arriving at the electrodes has been investigated and will be reported in a separate paper. An extension of the model to include the presence of negative ions inside the plasma sheath is currently in progress.

## ACKNOWLEDGMENTS

This work was supported by International Business Machines Corporation (Burlington) and by Wright Patterson Air Force base under Grant No. F33615-83-K-2340.

<sup>1</sup>The results described in this paper are also relevant for plasma reactors of different geometries as long as the thickness of the plasma sheaths is small compared to the electrode dimensions. Calculations show that for the electron (ion) number densities typical in low-pressure plasma reactors, the thickness of the plasma sheath is of the order of 1 mm. The model calculations presented here can also be extended to take into account the effect of reactor walls, etc., on the electrical characteristics of the reactor by adding circuit elements to the equivalent electric circuit model discussed in Sec. III.

<sup>2</sup>A. Garscadden and H. G. Emeleus, *Proc. Phys. Soc.* **79**, 535 (1962); A. Garscadden and P. Bletzinger, *Rev. Sci. Instrum.* **35**, 912 (1964).

<sup>3</sup>H. S. Butler and G. S. Kino, *Phys. Fluids* **67**, 1346 (1963).

<sup>4</sup>Keizo Suzuki, Ken Ninomiya, Shigeru Nishimatsu, and Sadayuki Okudaira, *J. Vac. Sci. Technol. B* **3**, 1025 (1985).

<sup>5</sup>R. T. C. Tsui, *Phys. Rev.* **168**, 107 (1968).

<sup>6</sup>H. R. Koenig and L. I. Maissel, *IBM J. Res. Dev.* **14**, 168 (1970).

<sup>7</sup>Chris M. Horwitz, *J. Vac. Sci. Technol. A* **1**, 60 (1983).

<sup>8</sup>A. J. van Roosemalen, W. G. W. van den Hoek, and H. Kalter, *J. Appl. Phys.* **58**, 653 (1985).

<sup>9</sup>C. B. Zarowin, *J. Electrochem. Soc.* **130**, 1144 (1983).

<sup>10</sup>K. Köhler, D. E. Horne, and J. W. Coburn, *J. Appl. Phys.* **58**, 3350 (1985).

<sup>11</sup>D. Bohm, in *The Characteristics of Electrical Discharges in Magnetic Fields*, edited by A. Guthrie and R. K. Wakerling (McGraw-Hill, New York, 1949), Chap. 3.

<sup>12</sup>This assumption is valid for electron energy modulation due to elastic interactions of electrons with atoms. [H. J. Oskam, *Philips Res. Repts.* **13**, 335 (1958)]. The energy modulation due to mutual charged particle interactions can be neglected for the assumed charge particle number densities of about  $10^{10} \text{ cm}^{-3}$ . Inelastic interactions between electrons and atoms involve only the small fraction of electrons in the high-energy tail of the electron energy distribution.

<sup>13</sup>The time constant  $\tau_D$  related to charged particle loss by ambipolar diffusion is, for an active plasma, given by  $\tau_D = (L/\pi)^2 (T_e/T_i) (D_+)^{-1}$ , where  $L$  is the distance between the electrodes,  $D_+$  is the diffusion coefficient of the ions, and  $T_e$  and  $T_i$  are the electron and gas temperatures, respectively.

<sup>14</sup>D. W. Ernie and H. J. Oskam, Final Technical Report, IBM, 1985.

<sup>15</sup>An extension of the Bohm sheath criterium to a surface biased slightly negative with respect to a plasma showed that this assumption is valid to within 5% for the smallest sheath voltage encountered in the present model (R. W. Carlson, Ph. D. thesis, University of Minnesota 1966).

<sup>16</sup>The ion current density is determined by the plasma density  $n_0$  at the interface between the plasma and the pre-sheath, the electron temperature, and the ion velocity, which is given by Bohm's criterium. The electron current density is determined by the plasma density  $n_0$ , the electron temperature, and the voltage across the sheath. Therefore, for a fixed potential between the plasma and the electrode, a nonzero value of the electric field at the sheath edge will only result in a slightly thinner plasma sheath and, thus, in a smaller transit time of the positive ions across the sheath.

<sup>17</sup>The fraction of electrons able to reach the electrodes for the sheath voltages encountered in the model is very small. The influence of this electron loss on the Boltzmann density distribution of the electrons in the sheath is very small (R. W. Carlson, Ph.D. thesis, University of Minnesota 1966).

<sup>18</sup>The potential difference between the electrode and the plasma is  $V_s$ . Therefore, the potential across the plasma sheath is  $(V_s - V_1)$ , where  $V_1$  is the potential across the pre-sheath in Bohm's model (Fig. 2). In the present model it is assumed that  $T_e$  is independent of time. Therefore,  $V_1$  can be omitted in Eqs. (1) and (2).

<sup>19</sup>R. H. Bruce, *J. Appl. Phys.* **52**, 7064 (1981).

Journal of Applied Physics is copyrighted by the American Institute of Physics (AIP). Redistribution of journal material is subject to the AIP online journal license and/or AIP copyright. For more information, see <http://ojps.aip.org/japo/japcr/jsp>  
Copyright of Journal of Applied Physics is the property of American Institute of Physics and its content may not be copied or emailed to multiple sites or posted to a listserv without the copyright holder's express written permission. However, users may print, download, or email articles for individual use.



Journal of Applied Physics is copyrighted by the American Institute of Physics (AIP). Redistribution of journal material is subject to the AIP online journal license and/or AIP copyright. For more information, see <http://ojps.aip.org/japo/japcr/jsp>